HHS Public Access

Author manuscript

Neuroscience. Author manuscript; available in PMC 2017 December 17.

Published in final edited form as:

Neuroscience. 2016 December 17; 339: 402–417. doi:10.1016/j.neuroscience.2016.10.023.

REPERTOIRE OF MESOSCOPIC CORTICAL ACTIVITY IS NOT REDUCED DURING ANESTHESIA

ANTHONY G. HUDETZ[a,*], **JEANNETTE A. VIZUETE**[b], **SIVESHIGAN PILLAY**[c], and **GEORGE A. MASHOUR**[a]

[a]Department of Anesthesiology, Center for Consciousness Science, Neuroscience Graduate Program, University of Michigan, Ann Arbor, MI, United States

[b]Department of Anesthesiology, Medical College of Wisconsin, Milwaukee, WI, United States

[c]Department of Psychiatry, University of Wisconsin-Madison, Madison, WI, United States

Abstract

Consciousness has been linked to the repertoire of brain states at various spatiotemporal scales. Anesthesia is thought to modify consciousness by altering information integration in cortical and thalamocortical circuits. At a mesoscopic scale, neuronal populations in the cortex form synchronized ensembles whose characteristics are presumably state-dependent but this has not been rigorously tested. In this study, spontaneous neuronal activity was recorded with 64-contact microelectrode arrays in primary visual cortex of chronically instrumented, unrestrained rats under stepwise decreasing levels of desflurane anesthesia (8%, 6%, 4%, and 2% inhaled concentrations) and wakefulness (0% concentration). Negative phases of the local field potentials formed compact, spatially contiguous activity patterns (CAPs) that were not due to chance. The number of CAPs was 120% higher in wakefulness and deep anesthesia associated with burst-suppression than at intermediate levels of consciousness. The frequency distribution of CAP sizes followed a power–law with slope −1.5 in relatively deep anesthesia (8–6%) but deviated from that at the lighter levels. Temporal variance and entropy of CAP sizes were lowest in wakefulness (76% and 24% lower at 0% than at 8% desflurane, respectively) but changed little during recovery of consciousness. CAPs categorized by *K*-means clustering were conserved at all anesthesia levels and wakefulness, although their proportion changed in a state-dependent manner. These observations yield new knowledge about the dynamic landscape of ongoing population activity in sensory cortex at graded levels of anesthesia. The repertoire of population activity and self-organized criticality at the mesoscopic scale do not appear to contribute to anesthetic suppression of consciousness, which may instead depend on large-scale effects, more subtle dynamic properties, or changes outside of primary sensory cortex.

[*]Corresponding author. Address: University of Michigan, Department of Anesthesiology, 1150 West Medical Center Drive, 7433 Medical Science Building 1, Ann Arbor, MI 48109-5615, United States. Fax: +1-734-764-9332. ahudetz@med.umich.edu (A. G. Hudetz).

DISCLOSURE OF FUNDING

National Institute of General Medical Sciences of the National Institutes of Health, Bethesda, Maryland, USA, Award Number R01-GM056398

Keywords

consciousness; anesthesia; information integration; criticality; synchrony; avalanche

INTRODUCTION

Cognitive functions are instantiated by transient neuronal ensembles organized at multiple spatial scales, from individual neurons, to neuronal populations, to large-scale networks (Werner, 2009b; Bressler and Menon, 2010). At the macroscopic level of field potentials such as the EEG, spatial patterns of electrical activity form metastable landscapes of sub-second duration, so-called microstates, that are associated with conscious, reportable thoughts or “mind states” (Lehmann et al., 1998). Using functional magnetic resonance imaging (fMRI) or voltage indicator imaging, dynamic patterns of local activity occur in wakefulness and anesthesia (Scott et al., 2014). At a smaller scale, neuronal populations in the cortex display stereotypic firing sequences that sample a relatively fixed repertoire of activity patterns as building blocks of the neuronal code; the patterns that occur during spontaneous ongoing activity resemble those evoked by somatosensory or auditory sensory stimulation (Luczak et al., 2009, 2015). In the visual cortex, spatiotemporal correlations of spikes are similar during spontaneous ongoing activity and during the presentation of natural visual scenes, suggesting that the sensory input triggers intrinsic circuit dynamics rather than generating stimulus-specific structure (Fiser et al., 2004). These and other observations (Shew et al., 2009) suggest that, even in the absence of exogenous stimuli, correlated spontaneous activity carries important information about the functional dispositions of local circuits.

An important outstanding question is how the repertoire of intrinsic activity patterns may be altered when the state of consciousness is modulated, as occurs, for example, during general anesthesia. The repertoire of states that the brain accesses over time has been hypothesized to be an essential determinant of the brain’s information capacity and its level of consciousness (Oizumi et al., 2014). A reduction in the brain’s large-scale network repertoire may explain reduced level of consciousness in dreamless sleep (Tononi, 2012) and anesthesia (Alkire et al., 2008). Conversely, its increase may be permissive for the psychedelic state (Carhart-Harris et al., 2014).

Experimental tests of the repertoire hypothesis are scarce (Barttfeld et al., 2015; Hudetz et al., 2015a) and most investigations have focused on patterns of connectivity and dynamics in large-scale brain networks (Boveroux et al., 2010; Martuzzi et al., 2010; Murphy et al., 2011; Schrouff et al., 2011; Barrett et al., 2012; Hudetz, 2012; Liu et al., 2012; Lee et al., 2013; Monti et al., 2013; Alonso et al., 2014; Blain-Moraes et al., 2014; Maksimow et al., 2014; Mashour, 2014; Nasrallah et al., 2014; Pal et al., 2015; Palanca et al., 2015; Sarasso et al., 2015; Hudetz et al., 2015a; Guldenmund et al., 2016; Tagliazucchi et al., 2016; Warnaby et al., 2016). Neuronal synchrony or dynamics at the spike or population level during general anesthesia have received considerably less attention (Sleigh et al., 2009; Lewis et al., 2012; Sellers et al., 2013, 2015; Hudson et al., 2014; Vizuete et al., 2014; Hudetz et al., 2015b). Understanding the repertoire of mesoscopic patterns of neural synchronization in local

circuits will be critical to bridge molecular effects of anesthetic binding to macroscopic neural, cognitive, and behavioral phenomena.

Mesoscopic dynamic patterns of neuronal population activity can be captured by local field potentials (LFPs) recorded with high-density microelectrode arrays. During spontaneous ongoing activity, neuronal population firing is closely correlated with the negative phase of the LFP, mainly due to synchronous dendritic depolarization of the population at a time scale that corresponds to the integration time of neurons – approximately 10 ms (Gabernet et al., 2005). The negative phases of LFPs (nLFPs) form spatiotemporal patterns whose size distribution follows scale-free (power–law) distribution (Beggs and Plenz, 2003), suggesting the presence of self-organized criticality (Werner, 2009a). The diversity of nLFP patterns serves as a measure of the brain's state repertoire that may, in turn, correlate with the state of consciousness. Dose-dependent effects of anesthetics on this repertoire associated with the loss or return of consciousness have not been determined.

To address this gap of knowledge, we recorded spontaneous ongoing LFP activity using 64-site silicone microelectrode arrays in the rat cerebral cortex *in vivo* at four anesthetic levels and wakefulness. We chose to record in primary visual cortex in order to enable comparison with our prior work (Vizuete et al., 2012, 2014; Hudetz et al., 2015b). Although neuronal activity in the primary visual cortex may not be sufficient, it is necessary to form conscious visual experience (Koch et al., 2016). The pattern of spontaneous neuronal activity in this region is modulated by bottom-up and top-down influences that shape the contents and quality of conscious visual experience (Cauller, 1995; Lamme and Roelfsema, 2000; Hudetz and Mashour, 2016).

For anesthesia, we chose desflurane, a clinically used inhalational agent that equilibrates rapidly (Eger and Johnson, 1987) and therefore allows more precise control of steady-state anesthesia level. We adjusted the anesthetic level from deep anesthesia to wakefulness in a step-wise manner while the animal regained consciousness.

We found that nLFPs formed stereotypic, contiguous activity pattern (CAP) formations that could not be accounted for by chance and whose size distribution followed power–law. Surprisingly, the repertoire of CAPs did not change when the animals regained consciousness although the proportion of frequency of occurrence of various CAPs changed in a state-dependent manner. The entropy of CAPs was also lowest in wakefulness. These observations yield fundamental new knowledge about the dominant spatial forms of spontaneous ongoing population activity in the rat visual cortex. The study reveals a dose-dependent effect of anesthesia on the temporal distribution of local activity patterns, while highlighting the invariance of their spatial repertoire despite the change in state of consciousness.

EXPERIMENTAL PROCEDURES

The experimental procedures and protocols were reviewed and approved by the Institutional Animal Care and Use Committee. All procedures conformed to the *Guiding Principles in the Care and Use of Animals* of the American Physiologic Society and were in accordance with

the *Guide for the Care and Use of Laboratory Animals* (National Academy Press, Washington, D.C., 2011). All efforts were made to minimize the number of animals used and their suffering.

Animal preparation

The surgical protocol has been previously described (Vizuete et al., 2012, 2014; Pillay et al., 2014). Briefly, 12 adult male Sprague–Dawley rats (260–440 gm) were chronically implanted with microelectrode arrays (Neuronexus Technologies, Inc., Ann Arbor, MI) for extracellular recording of the monocular region of the primary visual cortex (V1M, 7.0 mm posterior, 3.0–3.5 mm lateral to Bregma) (Paxinos and Watson, 1998). The microelectrode arrays had 64-contacts arranged as a planar 8 × 8 matrix (eight shanks, each with eight contacts) with a 200-μm contact spacing in both directions. The top recording sites were near the cortical surface in layer 1 and bottom recording sites were putatively in layers 5–6. The contacts were oriented in the sagittal plane and spanned the entire depth of the cortex. For reference, we used a stainless steel screw in the parietal cortex of the opposite hemisphere (4.0 mm posterior, 2.0 mm lateral, relative to bregma). The rats were allowed to recover for several days after surgery.

On the day of the experiment, the rat was placed in a ventilated anesthesia chamber where it could freely move. The room was darkened and the rat was allowed ~45 min to accommodate to the environment. Desflurane was applied in the sequence of 8%, 6%, 4%, 2% and 0% inhaled concentrations (added to 30% O_2 in N_2) for 45–50 min at each level. Vapor concentrations in the anesthesia chamber were continuously monitored (POET IQ2, Criticare Systems, Waukesha, WI, USA). During anesthesia, the core body temperature was rectally monitored (model 73A, YSI, Yellow Springs, OH, USA) and maintained at 37°C with subfloor radiant heat.

The 64-channel headstage preamplifier (ZC64 ZIF-Clip, Tucker-Davis Technologies, Alachua, FL, USA) was connected while the rat was under 8% desflurane anesthesia. At each anesthetic level, extracellular activity was recorded for 10 min after 15 to 20-min equilibration. LFPs were digitally sampled at 1000 Hz and band-pass filtered at 0.3–500 Hz (Cerebus, Blackrock Microsystems, Salt Lake City, UT, USA).

Data analysis

Ten minutes of LFP signals were filtered at 4–60 Hz using 1st-order Butterworth analog filter. Sections of data that contained large-amplitude artifacts, usually due to movement during wakefulness, were removed across all channels. Valid data were truncated to 6 min duration in each condition. The signals were then down-sampled to 100 Hz (in some cases, 200 Hz) yielding data series at 10 ms (5 ms) resolution. The ideal temporal resolution of nLFP events depends on the distance of recording sites (Beggs and Plenz, 2003); with 200-μm spacing, 10 ms is optimal and the cross-talk at this distance in the frequency band of interest is negligible. Following the method of (Petermann et al., 2009), the time stamps of negative signal deviations in excess of 2 standard deviations (SD) or 3 SD from the mean of each channel were determined yielding a multivariate binary time series of negative LFP events (nLFPs). The latter procedure was performed using a 2-s sliding window in order to

minimize the biasing effect of slow changes in LFP amplitude within the same condition. Data with absolute value greater than 6 SD were removed as artifacts. Simultaneous LFP deflections at more than half of the recording sites were rare, indicating that a distant source of activity from the reference electrode did not contaminate the nLFPs.

The multivariate binary time series were then analyzed for the spatial distribution of temporally correlated nLFPs. At each time point, most nLFPs appeared to aggregate into compact, contiguous clusters suggesting locally synchronous population activity. Because synchronous field activity is the hallmark of anesthetized and sleep states, we analyzed the size, frequency, and form of spatially connected nLFP clusters, from here on called contiguous activity patterns or CAPs. CAPs were determined using the Matlab command bwconncomp using eight neighbors (*x*, *y* and diagonal directions). As explained in the following, to exclude clusters formed by chance association, only CAPs with size greater than two were considered. Most time points contained only one large CAP. To avoid bias, the largest CAP from each time point was used.

The size distribution N(s) of the CAPs was determined and plotted on a log–log scale. A power–law equation of the form $N(s) \sim s^a$ was fitted to the data by linearizing the corresponding cumulative distribution function (White et al., 2008; Clauset et al., 2009) using the equation

$$\log(1-F(s))=(a+1)\log(s/s_0)$$

where the $F(s)$ is the cumulative distribution function of CAP size s and s_0 is the minimum cluster size.

To determine the most typical distinct CAP formations, the *K*-means method was applied at K=12, 24, 48, and 96 with the option of “cityblock” distance measure. The nLFP time series obtained in the five conditions were concatenated so that the same cluster types can be identified across the conditions. *K*-means was based on the size, centroid coordinates, eccentricity, and orientation of the CAPs at each time point (size >2). The CAPs within each type, as predicted by the *K*-means procedure, were averaged across the entire time series to yield a probabilistic representation of each type. The frequencies of each cluster type in the five conditions were then compared.

K-means clustering was also performed using a set of objectively selected features obtained by dimensional reduction of the data with principal components analysis (PCA). PCA was applied to the multichannel nLFP binary time series concatenated across five conditions and *K*-means was performed using the six largest principal components as features.

The entropy S of CAPs was calculated from their size distribution using an unbiased estimator (Moddemeijer, 1989) based on Shannon’s formula:

$$S=-p_i\sum\log(p_i)$$

where p_i is the probability of occurrence the CAP of size i (i>2) and the summation is for i. S was calculated separately for each state and animal.

We estimated the probability of CAPs forming by chance. The probability of k events from n Bernoulli trials is given by

$$P(n,k)=C(n,k)p^k(1-p)^{(n-k)}$$

where $C(n, k)$ is the binomial coefficient and p is the probability of an event. We assume that all events are independent. The trials can be sequential or can represent drawings from a set of size n. We are concerned with estimating the probability of co-occurrence of k events on n sites with the constraint that the events should occur at neighboring sites. Here, n is the number of recording sites and k is the CAP size. To estimate this probability, the binomial coefficients have to be modified to take the constraint into account. A treatment of selected combinations in a serial sample was presented by Muir (1902). However, we need further modification because the neighborhood constraints in our case are defined on the two-dimensional plane of electrode contacts. It can easily be seen that the proper combinations for the first few cluster sizes k on a square matrix set of size n are:

$$\begin{aligned} C(n,1) &= n \\ C(n,2) &= n \cdot 8/2! \\ C(n,3) &= n \cdot 8 \cdot 10/3! \\ C(n,4) &= n \cdot 8 \cdot 10 \cdot 12/4! \\ &\dots \end{aligned}$$

Clearly, the first event can occur at any of the n positions, the second neighboring event at eight positions surrounding the first event, the third neighboring event can occur at 10 positions, etc. In closed form for k>1:

$$C(n,k)=n/k! \cdot P[6+2(i-1)]$$

where in the product i runs from 2 to k. To aid the derivation of the above coefficients, we applied the simplifying assumption of periodic boundary conditions. If n is large and k is small, then this assumption does not cause a significant error. The average probability of an nLFP at any recording site was estimated as p= N/(T·n) where N is the number of the total nLFPs in a data sample, T is the sample duration (number of time points per condition, 24,000) and n is the number of sites, in this case, 64. $P(n, k)$ was then calculated for K=2, 3, 4, etc. $P(n, k)$ estimates the chance occurrence of CAP of size k at one time point.

Surrogate data were obtained by shifting the individual nLFP time series by a random integer with values between −100 and +100 drawn from a uniform distribution. Several methods of randomization to create surrogate data sets have been proposed (Grun, 2009). Shifting the entire time series of channels relative to each other is favored because it preserves the spectral characteristics of all time series while destroying their correlation structure. The choice of shift range was based on the time gaps between nLFP events.

To determine if the CAPs' distributions were due to higher-order correlations of the LFP signals, we generated a second set of surrogate signals that preserved both the amplitude spectra and the pair-wise correlations among the signals. Using the method of (Prichard and Theiler, 1994), LFP signals were Fourier-transformed and the phase of each frequency component was rotated by a uniformly distributed random number in the range of [0,pi), using the same phase rotation for all LFP channels. Applying the inverse Fourier transform yielded a phase-randomized signal with conserved power spectrum and pairwise correlations but absent higher-order correlations. Surrogate nLFPs were then obtained by thresholding and binarizing the phase-randomized LFP signals. The calculation was performed on 6 min of downsampled (100 Hz), filtered and normalized LFP data.

To quantify the spatial segregation tendency of the CAPs in five states, the x – *y* center coordinates of the CAPs were represented as a 40 × 40-pixel binary image. An entropy filter was applied to each image (entropyfilt.m, Matlab) that is used to extract a smooth, statistically clustered neighborhood. Each pixel of the filtered image contained the entropy value of the 9-by-9 neighborhood around each pixel of the original image. The resulting image was then thresholded at 0.85, 0.80, or 0.95 level to arrive at a binary representation of clustered CAP centers. The percentage of pixels that passed threshold was taken as an index of CAP center clustering.

Statistical analysis

The concentration-dependent effects of desflurane on the number of CAPs, wait times and cluster size were tested using repeated measures analysis of variance (RM-ANOVA) with the anesthetic concentration as within factor and the rat as subject followed by Tukey–Kramer all pair-wise multiple comparison (T-K) at alpha=0.05 level. The sphericity assumption for each RM-ANOVA was checked with Mauchly's test and was found violated. Therefore, Geisser–Greenhouse correction was applied and adjusted p values (Geisser–Greenhouse epsilon probability levels) were used. Statistical significance of deviation of cluster size distribution from power–law was tested with the Kolmogorov–Smirnov test (K–S). Sample sizes were determined based on previous experience. Blinding methods were not feasible because of the close involvement of all investigators in the experimental and analytical work. All calculations were performed using MATLAB 2011a (MathWorks, Natick, MA, USA). Statistical testing of group results was performed using NCSS 2007 (NCSS, Kaysville, UT, USA). The central tendency of all data is reported as arithmetic mean and standard deviation unless noted otherwise. Scatter plots show standard errors of the mean.

RESULTS

Negative LFPs reflect population spikes under anesthesia

We examined the spatiotemporal structure of LFP and extracellular unit activity recorded by 64-site silicone electrodes in visual cortex of twelve rats at four levels of desflurane anesthesia and wakefulness. The negative phases of the LFPs were closely correlated with bursts of extracellular spiking, which was most evident during burst suppression at the deepest level of anesthesia at 8% desflurane (Fig. 1). Reducing the concentration of anesthetic to 6%, 4% and 2%, made the spiking gradually more continuous but the

correlation with negative LFP phases was still discernible. These results justify the use of nLFP as an indicator of population activity across various anesthetic conditions.

The frequency spectra of LFPs under different conditions were similar with the exception that the low-frequency amplitude was gradually reduced as the anesthetic was withdrawn (Fig. 2). There was a significant linear trend in the peak amplitude vs. desflurane (p=0.0011, RM-ANOVA).

To obtain a binary representation of the LFP activity correlated with population spiking, we re-sampled the LFP at 100 Hz. At each time point, the LFP falling below a chosen threshold (1, 2 or 3 SD below the mean) was defined as an nLFP event and assigned a value of 1 in the corresponding time series.

nLFPs form stereotypic CAPs

nLFPs showed a strong tendency to form spatial clusters that changed their configuration frequently (Movie 1). We found that 88±15% of the nLFPs formed close aggregates or, as we refer to them, contiguous activity patterns (CAPs). By visual inspection, similar clustering of nLFPs occurred under anesthesia, although they were often separated by longer time gaps (Movie 2). Our main goal was then to determine if anesthesia altered the number and diversity of various forms CAPs. The latter was considered as a measure of the repertoire of population activity patterns or “states” the brain would enter over time.

CAPs larger than 2 do not form by chance

We examined analytically the probability that CAPs occurred by the chance association of nLFPs. Combining data from all experiments, the average probability of an nLFP to occur was 0.293±0.041. Using a combinatorial model (see Methods), we estimated the probability of the chance occurrence of a size-2 CAP (i.e., two adjacent nLFPs) as $78 \pm 24 \times 10^{-4}$ equivalent to 187±58 CAPs in a 4-min period. This was comparable to the actual number of size 2 clusters at 422±115 (mean and SEM over all experiments and conditions). The calculated probability of a size-3 CAP to occur by chance was $18 \pm 8 \times 10^{-5}$ equivalent to 4±2 CAPs in four minutes. This number was negligible compared to the 188±37 CAPs observed suggesting that CAPs larger than two could not be formed by chance but by correlated neuronal activity.

CAP size distribution follows power–law

To analyze the statistical distribution of CAP size in five states, nLFP data were combined from all animals and the number of CAPs (including sizes 1 and 2) was plotted as a function of CAP size (Fig. 3). The distributions at 8% and 6% desflurane followed a power–law as indicated by a linear relationship in the log–log plot with a slope close to −1.5 (N.S. vs. power– law distribution, K–S test, p values in the figure). The distributions deviated from power–law at lighter planes of anesthesia and wakefulness (p values in figure) due to a decrease in the proportion of large CAPs. In fact, the number of CAPs greater than 32 (half the number of recording sites) decreased from 834 to 164 between 8% and 0% desflurane, respectively. There was also a slight change in slope at −1.56 to −1.69. Random shuffling of

the nLFP time series relative to each quickly diminished the proportion of CAPs with size >2 and destroyed the power–law relationship consistent with the theoretical prediction.

Because thresholded stochastic processes can produce higher-order correlations and give rise to spurious power–law scaling that do not relate to self-organized criticality (Touboul and Destexhe, 2010), we examined whether the CAP distributions arose from higher-order correlations. By randomizing the phase of the LFP signals prior to thresholding, we generated surrogate LFP signals that had unchanged power spectrum and pair-wise correlations (Fig. 4) but were free from higher-order correlations. We found that the average pair-wise correlation coefficients of nLFPs derived from the surrogate signals were very similar to those obtained from of original signals in all states except at the deepest anesthetic level where the correlation was reduced after phase-randomization (p=00011, RM-ANOVA interaction term; p=0.00066, comparison at 8%). The power– law distribution of the surrogate CAPs was preserved in all states (Fig. 3). Therefore, the only state in which higher-order correlation may contribute to the CAP statistics is burst-suppression at 8% desflurane.

CAP size varies with the anesthetic level

A summary of the average number of CAPs (size >2) as a function of desflurane concentration from all animals is shown in Fig. 5. The U-shape dependence on anesthetic depth showed that significantly increased population activity at the deepest level of anesthesia (8%) and in wakefulness (0%) compared to intermediate anesthetic levels (p=0.0026, RM-ANOVA, T-K p<0.05). This demonstrates clearly that CAPs vary with levels of activity vs. levels of consciousness. The high number of CAPs at 8% desflurane was associated with burst-suppression that occurred in eight of 12 animals. The degree of burst-suppression was quantified by the burst-suppression ratio (BSR, Table 1). When the animals with BSR >3% were excluded, the number of CAPs at 8% desflurane was similar to that at 6% desflurane (see separate point in figure). Shuffling the nLFP data as described above diminished the number of CAPs. Similar dependence of CAP number on state were obtained when LFPs were thresholded at 2 SD or binned 5 ms confirming that the parameter choices did not qualitatively influence the results.

Variance and entropy of CAP size differ between wakefulness and deep anesthesia

As indicated in Table 1, rats 1–8 showed significant burst-suppression at the 8% desflurane. A good example is shown in Fig. 1. Burst-suppression also gives rise to a large fluctuation in CAP size. As seen in Fig. 6, the fluctuations were quite large at 8% desflurane in rats 1–8. The fluctuations were small in the absence of bursting (rats 9–12).

In most of the animals, the fluctuations were the smallest in wakefulness, which is consistent with the well-known small-amplitude, fast EEG or LFP patterns. In the intermediate states (6%–2% desflurane), the fluctuations showed greater individual variability. A general linear relationship between CAP size variance and desflurane concentration was significant (p=0.0014, RM-ANOVA, Fig. 7A). A similar, nearly monotonic relationship with desflurane concentration was observed for the entropy of CAP sizes (p=0.0005, RM-ANOVA). As shown in Fig. 7B, entropy was the lowest in wakefulness compared to all other states.

Classification of CAP types

Visual inspection suggested that CAPs formed distinct recurrent forms. To characterize the distribution of the different forms in five conditions (four states of anesthesia and wakefulness), we performed *K*-means clustering of CAPs using their size, center coordinates, eccentricity, and orientation as clustering features. It was determined that eccentricity and orientation did not add to the quality of classification. Due to the probabilistic nature of CAP formations, and because the distribution of nLFPs in the array is not Gaussian, we did not attempt to determine how many distinct forms there might be. Instead, we performed *K*-means clustering at different chosen *K* values (*K*=12, 24, 48, and 96) and compared the distributions among the five conditions at each *K*.

Fig. 8 illustrates the average landscapes of classified CAPs for *K*=12. There was an approximately fourfold (3.9±2.0) variation in the percentage of CAPs between the most and the least frequent clusters suggesting a substantially unequal frequency of occurrence of the CAPs.

The lifetime of CAPs that belonged to each cluster was short. Cluster membership can change due to noise if the number of clusters *K* is high; this effect is reduced at small *K* that yields maximally distinct cluster shapes. Even with *K*=12, persistence of the same cluster type for two or more time points was less than 1% (0.73±0.32%, *K*=12, all data combined). In other words, CAPs were switching spatial configuration on a time scale of as short as 10 ms.

Because the choice of clustering features was arbitrary, we validated the results with an alternative approach. Based on prior studies (Hudson et al., 2014), we chose to apply dimensional reduction of the data using PCA. When PCA was applied to the temporally concatenated multichannel nLFP data, we were able to explain, on average, 72% (range 65–92%) of variance using only six principal components. After reapplying *K*-means clustering with the six principal components as a new feature vector, we obtained results that were practically identical to those obtained with the previously used features.

CAP type frequencies are state-dependent

A fundamental question of our study was if the spatial landscape of CAPs was altered by the anesthetic state. Does the number of CAPs of each cluster change with anesthesia? Fig. 9A shows that, regardless of the chosen *K* value, the same clusters were present in each state. However, it was still possible that the distribution of CAPs across the same clusters was different in each state. To examine this, we sorted the clusters in the order of the number of CAPs contained. Fig. 9B suggests that a redistribution of CAP numbers indeed occurred as a function of state. Although illustrative, this result could not be tested statistically because the CAP clusters were not readily comparable among the animals and clustering of concatenated nLFP data from all rats and all conditions was not computationally tractable.

To test our hypothesis a different way, we calculated the SD of the number of CAPs across the *K*-means clusters (*K*=12) and all rats. We found that the SD were substantially higher in the two extreme states (92.9 and 105.4 at 8% and 0% desflurane, respectively) than at the intermediate levels (27.7, 28.7, and 32.3 at 6%, 4% and 2%, respectively) suggesting that the

number of CAP types were indeed redistributed as a function of state such that they were more heterogeneous during wakefulness and burst suppression than at the intermediate levels. Repeating the SD calculations in each rat separately confirmed that the difference was statistically significant (p=0.0023, RM-ANOVA, p<0.05, T-K).

CAP centroids are more segregated in wakefulness

To gain further information about the clustering tendency of CAPs in each state, we examined the spatial distribution of their $x-y$ center coordinates. The centers tended to localize in various regions of the recording plane that changed with the anesthetic state. To quantify the clustering tendency, we calculated the percentage of center sites that aggregated together with high probability at a select entropy threshold (see methods). Fig. 9C shows that the percentage of clustered CAP centers was the highest at 0% desflurane and significantly different from those at 6% and 4% (p=0.0323, RM-ANOVA, p<0.05, T-K). That is, the CAPs were the most localized during wakefulness. This difference was relatively insensitive to the threshold selections used to define the clusters. Individual maps of the center coordinates are shown in Fig. 10.

DISCUSSION

How, precisely, general anesthetics suppress consciousness has been an elusive problem for approximately 170 years. Anesthetics are known to suppress spontaneous ongoing neuronal activity in a dose-dependent manner (Robson, 1967; Ikeda and Wright, 1974; Armstrong-James and George, 1988; Angel, 1991; Ogawa et al., 1992; Villeneuve and Casanova, 2003; Hentschke et al., 2005; Sellers et al., 2013). However, the critical neuronal events that account for the suppression of consciousness remain unknown (Alkire et al., 2008; Mashour, 2014; Meyer, 2015). Few studies have explored the dose-dependent effect of anesthetics on cortical neuronal activity or connectivity at the level of units or LFPs (Sellers et al., 2013, 2015; Hudson et al., 2014; Raz et al., 2014; Vizuete et al., 2014).

Understanding the mechanisms of state-dependent changes in level of consciousness requires a principled approach based on a theoretical framework (Crick et al., 2004). For example, the Integrated Information Theory (Tononi et al., 2016) implies that the repertoire of states that the brain accesses over time is an essential determinant of the brain's information capacity and level of consciousness (Oizumi et al., 2014), a reduction in the brain's state repertoire may explain reduced level of consciousness during anesthesia (Alkire et al., 2008). Empirical findings from large-scale network connectivity in the brain are consistent with this notion (Barttfeld et al., 2015; Hudetz et al., 2015a).

Another fundamental postulate is that consciousness occurs in the brain in the dynamic regime of self-organized criticality (Werner, 2009a) often indicated by power–law relationships (Bak and Paczuski, 1995; Beggs and Plenz, 2003) although not without critique (Beggs and Timme, 2012). However, power–laws of neuronal population events are also present in anesthetized animals and in vitro preparations (Massobrio et al., 2015) and systematic assessment their state-dependence has been scarce (Ribeiro et al., 2010). On a larger spatial scale, Lee et al. (2010) investigated the effect of propofol anesthesia in healthy volunteers using multichannel electroencephalography and found that global scale-free

organization (indicated by the power–law of connection times) was preserved across all states of consciousness in spite of a significant reduction in the number of network connections under anesthesia. Subsequently, Hudson et al. (2014) investigated the dynamics of intracortical and intrathalamic field potentials in rats during stepwise recovery from isoflurane anesthesia and found that LFP power followed an orderly sequence of discrete metastable states that persisted for minutes as the animals approached the state of consciousness. This suggests that, of the vast number of potential neuronal activity states, the brain enters a restricted subspace of states en route to consciousness. Likewise, Solovey et al. (2015) investigated critical phenomena in multichannel EEG recording across the entire hemisphere of monkeys anesthetized with propofol or ketamine +medetomidine and found that loss of consciousness was associated with the stabilization of cortical dynamics. Finally, Tagliazucchi et al. found that large-scale dynamics based on fMRI departed from critical regime during propofol-induced unconsciousness (Tagliazucchi et al., 2016).

We found that spontaneous population events, nLFPs, in rat visual cortex form stereotypic, contiguous spatial clusters (CAPs) that could not be accounted for by chance, suggesting that they were formed by the synchronization of local neuronal populations. The size, number, and configuration of CAPs changed with the anesthetic level but the repertoire of CAP types was unchanged. The CAPs showed relatively low variance in size, low entropy, and stronger tendency to localize in the wakeful state. However, these parameters changed insignificantly near the transition from the unconscious to conscious state, suggesting that these changes were not correlated with the state of consciousness *per se*.

The invariance of the repertoire of CAPs in anesthesia relative to wakefulness was unexpected given the presumption that the brain's state repertoire is an essential determinant of the level of consciousness – a fundamental postulate of the Integrated Information Theory (Tononi et al., 2016). Our finding does not refute the proposition that the state repertoire – a putative indicator of the brain's information capacity, is *necessary* for the conscious state. Our results do suggest the possibility that the contraction of large-scale network repertoire is not reducible to a contraction of mesoscopic spatial repertoires. The data also focus future investigation on whether the sparsification of population events within a given time frame—or, alternatively, the functional uncoupling of those events with events in other areas of the cortex—is the driving factor for reduced large-scale network repertoire. This has been measured by the configurations of large-scale intrinsic networks by fMRI. Using this modality, anesthesia was found to have a significant effect in both rodents and primates, albeit with a different anesthetic agent, propofol (Barttfeld et al., 2015; Hudetz et al., 2015a). Obviously, our finding hinges on the definition of the repertoire, and the diversity of CAPs derived from nLFPs is only one possible measure of the local population repertoire. Examination of the temporal evolution of CAPs using sliding windows (Hudson et al., 2014) could be a natural extension of the work in the future. This may include conditioning the probability of each CAP on its predecessor(s), perhaps similar to the definition of the dynamic complexity measure phi* (Oizumi et al., 2016). Alternatively, it is possible that correlated activity of individual neurons may be more informative regarding anesthesia-dependent changes in the repertoire of brain states (Pillay et al., 2014).

The power–law distribution of CAPs with a slope of −1.5 – a putative indicator of self-organized criticality, was prevalent under deep anesthesia; the distribution began to deviate from power–law with the recovery of consciousness. This suggests that anesthetic unconsciousness could not be accounted for by a deviation from criticality, as the latter did not occur in anesthesia. The result is consistent with the finding from spike avalanches in ketamine+xylazine-anesthetized cats (Ribeiro et al., 2010). Also, power laws in nLFP size suggesting the presence of criticality were found in both awake and anesthetized animals (Petermann et al., 2009; Massobrio et al., 2015), although usually not in the same preparation. In contrast, a recent voltage indicator imaging study suggested that large-scale cortical dynamics in pentobarbital-anesthetized mice deviated from power–law but returned after recovery of wakefulness (Scott et al., 2014). Finally, an fMRI study using graph analysis of large-scale intrinsic networks showed that power–law distribution of node-degree was unchanged in propofol-anesthetized human subjects as compared to wakefulness (Liu et al., 2014). Although the reason for these discrepancies is unclear, differences in the modality and scale of measurements (spikes vs. LFPs vs. BOLD fMRI) as well as the difference in the investigated anesthetic agents (inhalational vs. intravenous, GABA vs. NMDA targets, etc.) may have played a role. Due to the size of our electrode arrays, the true extent of CAPs could not be determined; they could have extended to a larger scale than recorded here, at which their power–law behavior may have been different. There is an obvious tradeoff between large-scale field recordings across the cortical surface (Scott et al., 2014) vs. cortical depth recordings at a smaller scale. Also, optical techniques cannot measure neuronal population activity at millisecond temporal resolution.

It is also important to point out that our analysis of CAPs was different from the analysis of neuronal avalanches that are also based on nLFPs (Beggs and Plenz, 2003; Petermann et al., 2009; Hahn et al., 2010). Avalanches are temporally extended events that consist of a series of nLFPs occurring at frequently different locations. The quantification of avalanches necessarily ignores the spatial configurations of nLFPs since they generally change with each time step. Given the combinatorial explosion of temporally extended potential nLFP patterns and the limitation for sufficiently sampling these patterns at several steady state anesthetic levels in the same experiment, an analysis of the repertoire of avalanches seems statistically prohibitive. Instead, we quantified the spatial repertoire of nLFPs clusters at individual time points as “unitary states” similar to that used for the classification of coincident spike patterns (Grun et al., 2002). In this regard, our approach was similar to the EEG “microstate” analysis pioneered by Lehmann and colleagues (Lehmann et al., 1998; Koenig et al., 2002) with the exception that their analysis was based on multi-channel scalp EEG. At the macroscopic scale of EEG, the average duration of microstates was approximately an order of magnitude longer than at the scale of nLFPs.

The nLFPs also correlate nicely with the population spiking of neurons. The effect of desflurane anesthesia on spike correlations was previously investigated (Vizuete et al., 2012, 2014; Hudetz et al., 2015b). However, CAPs could not be analyzed from spike data directly because spikes were generally present only at approximately half of contacts of the electrode array. In contrast, LFPs could be consistently recorded from all electrode sites.

The finding of low entropy of CAP sizes in wakefulness is interesting as it suggests that this state assumes more order in spite of a similar repertoire of CAPs. In a recent study using spike-based metrics, we found that integration and complexity of neuronal interactions were relatively low in anesthesia and high in wakefulness (Hudetz et al., 2015b). While this may appear to be a conflicting result, weaker neuronal interactions in anesthesia may allow the CAP sizes to be more random, equivalent to higher entropy, with the converse being true in wakefulness. Nevertheless, spike and CAP entropies may be different and the entropy of CAP type (as opposed to size) was not calculable due to the relatively small sample size. Also, at first sight, the change in entropy may suggest a commensurate change in the repertoire. However, the reduction in the entropy of CAP sizes in wakefulness could be due to a more homogeneous distribution even if the repertoire itself (the number of unique CAPs in each condition) is unchanged. The gradual loss of large CAPs during light anesthesia and wakefulness may be due to the frequent interruption of newly forming CAPs - consistent with the traditional notion of LFP desynchronization. The temporal development of individual CAPs at a higher sampling rate than used here could be investigated in the future.

We also found a change in the clustering of CAP centers that were more segregated in wakefulness (0% desflurane). Raz et al. (2014) found that cross-modal sensory responses were preferentially attenuated by isoflurane in superficial cortex where top-down associational projections terminate. We expected to see a change in laminar pattern of the centroids with anesthetic depth but found no systematic trend, apparently because the changes were too different in each animal. Of course, the laminar distribution of anesthetic modulation may be different during spontaneous ongoing activity from that during sensory stimulation.

Interestingly, the overall number of CAPs was high in both wakefulness and in deep anesthesia as compared to the intermediate anesthesia levels. This observation underlines the importance of examining graded states of anesthesia. Comparing neuronal activity between wakefulness and deep anesthesia alone can miss the important changes in neuronal activity associated with loss or return of consciousness that occur at intermediate anesthetic levels (4.3% desflurane, (Imas et al., 2005)). Why the nLFP activity is high in deep anesthesia is explained by the presence of burst-suppression that occurred in 8 of 12 animals in our study. Burst-suppression is a distinct condition in which neuronal activity semi-periodically alternates between highly active and profoundly inactive states (Rampil et al., 1991; Steriade et al., 1994; Lukatch et al., 2005; Kenny et al., 2014). Bursting is a hyperexcited state (Hartikainen et al., 1995; Detsch et al., 2002; Hudetz and Imas, 2007; Kroeger and Amzica, 2007) in which the overall (time-averaged) level of spontaneous activity is high. This demonstrates that the number and clustering of CAPs in the visual cortex correlates with the level of neuronal activity rather than with level of consciousness. Not all anesthetics cause burst-suppression and those that do may produce distinct burst-suppression patterns (Kenny et al., 2014). Finally, the similarity of neuronal activity during wakefulness and bursts (Up states) has prompted the intriguing question of whether the Up states correspond to fragments of wakefulness (Destexhe et al., 2007). Considering the average duration of Up states of a few 100 ms and that conscious experience requires unimpeded stimulus processing for approximately 100– 200 ms (Bachmann, 1998; Hudetz, 2006), this possibility merits further investigation.

In summary, our results show that population activity in rat visual cortex forms compact, dynamically changing activity patterns, whose stereotypical forms are conserved at all anesthetic levels. The statistical distribution of these activity patterns remains close to power law during the transition from unconscious to conscious states. The results suggest that the mesoscopic repertoire of local brain states in visual cortex does not change in anesthesia. Of course, the contents of consciousness in nonvisual sensory and other nonsensory modalities may not solely depend on the state repertoire of visual cortex. Consciousness in general may depend on large-scale dynamics, more subtle interactions in local circuits, or higher-order association areas of the cerebral cortex.

Supplementary Material

Refer to Web version on PubMed Central for supplementary material.

Acknowledgments

Research reported in this publication was supported by the National Institute of General Medical Sciences of the National Institutes of Health, Bethesda, MD under Award Number R01-GM056398. The content is solely the responsibility of the authors and does not necessarily represent the official views of the National Institutes of Health. The insightful, constructive comments of two anonymous reviewers are greatly appreciated.

Abbreviations

CAPs	contiguous activity patterns
fMRI	functional magnetic resonance imaging
LFPs	local field potentials
nLFPs	negative phases of LFPs
PCA	principal components analysis

References

Alkire MT, Hudetz AG, Tononi G. Consciousness and anesthesia. Science. 2008; 322:876–880. [PubMed: 18988836]

Alonso LM, Proekt A, Schwartz TH, Pryor KO, Cecchi GA, Magnasco MO. Dynamical criticality during induction of anesthesia in human ECoG recordings. Front Neural Circuits. 2014; 8:20. [PubMed: 24723852]

Angel A. The G. L. Brown lecture. Adventures in anaesthesia. Exp Physiol. 1991; 76:1–38. [PubMed: 2015066]

Armstrong-James M, George MJ. Influence of anesthesia on spontaneous activity and receptive field size of single units in rat Sm1 neocortex. Exp Neurol. 1988; 99:369–387. [PubMed: 3338529]

Bachmann T. Is conscious experience established instantaneously? Commentary on J.G. Taylor. Conscious Cogn. 1998; 7:149–156. [PubMed: 9690016]

Bak P, Paczuski M. Complexity, contingency, and criticality. Proc Natl Acad Sci U S A. 1995; 92:6689–6696. [PubMed: 11607561]

Barrett AB, Murphy M, Bruno MA, Noirhomme Q, Boly M, Laureys S, Seth AK. Granger causality analysis of steady-state electroencephalographic signals during propofol-induced anaesthesia. PLoS One. 2012; 7:e29072. [PubMed: 22242156]

Barttfeld P, Uhrig L, Sitt JD, Sigman M, Jarraya B, Dehaene S. Signature of consciousness in the dynamics of resting-state brain activity. Proc Natl Acad Sci U S A. 2015; 112:887–892. [PubMed: 25561541]

Beggs JM, Plenz D. Neuronal avalanches in neocortical circuits. J Neurosci. 2003; 23:11167–11177. [PubMed: 14657176]

Beggs JM, Timme N. Being critical of criticality in the brain. Front Physiol. 2012; 3:163. [PubMed: 22701101]

Blain-Moraes S, Lee U, Ku S, Noh G, Mashour GA. Electroencephalographic effects of ketamine on power, cross-frequency coupling, and connectivity in the alpha bandwidth. Front Syst Neurosci. 2014; 8:114. [PubMed: 25071473]

Boveroux P, Vanhaudenhuyse A, Bruno MA, Noirhomme Q, Lauwick S, Luxen A, Degueldre C, Plenevaux A, Schnakers C, Phillips C, Brichant JF, Bonhomme V, Maquet P, Greicius MD, Laureys S, Boly M. Breakdown of within- and between-network resting state functional magnetic resonance imaging connectivity during propofol-induced loss of consciousness. Anesthesiology. 2010; 113:1038–1053. [PubMed: 20885292]

Bressler SL, Menon V. Large-scale brain networks in cognition: emerging methods and principles. Trends Cogn Sci. 2010; 14:277–290. [PubMed: 20493761]

Carhart-Harris RL, Leech R, Hellyer PJ, Shanahan M, Feilding A, Tagliazucchi E, Chialvo DR, Nutt D. The entropic brain: a theory of conscious states informed by neuroimaging research with psychedelic drugs. Front Hum Neurosci. 2014; 8:20. [PubMed: 24550805]

Cauller L. Layer I of primary sensory neocortex: where top-down converges upon bottom-up. Behav Brain Res. 1995; 71:163–170. [PubMed: 8747184]

Clauset A, Shalizi CR, Newman MEJ. Power–law distributions in empirical data. Siam Rev. 2009; 51:661–703.

Crick F, Koch C, Kreiman G, Fried I. Consciousness and neurosurgery. Neurosurgery. 2004; 55:273–281. discussion 281–272. [PubMed: 15271233]

Destexhe A, Hughes SW, Rudolph M, Crunelli V. Are corticothalamic 'up' states fragments of wakefulness? Trends Neurosci. 2007; 30:334–342. [PubMed: 17481741]

Detsch O, Kochs E, Siemers M, Bromm B, Vahle-Hinz C. Increased responsiveness of cortical neurons in contrast to thalamic neurons during isoflurane-induced EEG bursts in rats. Neurosci Lett. 2002; 317:9–12. [PubMed: 11750984]

Eger EI 2nd, Johnson BH. Rates of awakening from anesthesia with I-653, halothane, isoflurane, and sevoflurane: a test of the effect of anesthetic concentration and duration in rats. Anesth Analg. 1987; 66:977–982. [PubMed: 3631595]

Fiser J, Chiu C, Weliky M. Small modulation of ongoing cortical dynamics by sensory input during natural vision. Nature. 2004; 431:573–578. [PubMed: 15457262]

Gabernet L, Jadhav SP, Feldman DE, Carandini M, Scanziani M. Somatosensory integration controlled by dynamic thalamocortical feed-forward inhibition. Neuron. 2005; 48:315–327. [PubMed: 16242411]

Grun S. Data-driven significance estimation for precise spike correlation. J Neurophysiol. 2009; 101:1126–1140. [PubMed: 19129298]

Grun S, Diesmann M, Aertsen A. Unitary events in multiple single-neuron spiking activity: II. Nonstationary data. Neural Comput. 2002; 14:81–119. [PubMed: 11747535]

Guldenmund P, Gantner IS, Baquero K, Das T, Demertzi A, Boveroux P, Bonhomme V, Vanhaudenhuyse A, Bruno MA, Gosseries O, Noirhomme Q, Kirsch M, Boly M, Owen AM, Laureys S, Gomez F, Soddu A. Propofol-Induced Frontal Cortex Disconnection: A Study of Resting-State Networks, Total Brain Connectivity, and Mean BOLD Signal Oscillation Frequencies. Brain Connect. 2016

Hahn G, Petermann T, Havenith MN, Yu S, Singer W, Plenz D, Nikolic D. Neuronal avalanches in spontaneous activity in vivo. J Neurophysiol. 2010; 104:3312–3322. [PubMed: 20631221]

Hartikainen KM, Rorarius M, Perakyla JJ, Laippala PJ, Jantti V. Cortical reactivity during isoflurane burst-suppression anesthesia. Anesth Analg. 1995; 81:1223–1228. [PubMed: 7486108]

Hentschke H, Schwarz C, Antkowiak B. Neocortex is the major target of sedative concentrations of volatile anaesthetics: strong depression of firing rates and increase of GABAA receptor-mediated inhibition. Eur J Neurosci. 2005; 21:93–102. [PubMed: 15654846]

Hudetz AG. Suppressing Consciousness: mechanisms of general anesthesia. Semin Anesth Perioperative Med Pain. 2006; 25:196–204.

Hudetz AG. General anesthesia and human brain connectivity. Brain Connect. 2012; 2:291–302. [PubMed: 23153273]

Hudetz AG, Imas OA. Burst activation of the cerebral cortex by flash stimuli during isoflurane anesthesia in rats. Anesthesiology. 2007; 107:983–991. [PubMed: 18043067]

Hudetz AG, Mashour GA. Disconnecting consciousness: is there a common anesthetic end point? Anesth Analg. 2016

Hudetz AG, Liu X, Pillay S. Dynamic repertoire of intrinsic brain states is reduced in propofol-induced unconsciousness. Brain Connect. 2015a; 5:10–22. [PubMed: 24702200]

Hudetz AG, Vizuete JA, Pillay S, Ropella KM. Critical Changes in Cortical Neuronal Interactions in Anesthetized and Awake Rats. Anesthesiology. 2015b

Hudson AE, Calderon DP, Pfaff DW, Proekt A. Recovery of consciousness is mediated by a network of discrete metastable activity states. Proc Natl Acad Sci U S A. 2014; 111:9283–9288. [PubMed: 24927558]

Ikeda H, Wright MJ. Sensitivity of neurones in visual cortex (area 17) under different levels of anaesthesia. Exp Brain Res. 1974; 20:471–484. [PubMed: 4442483]

Imas OA, Ropella KM, Ward BD, Wood JD, Hudetz AG. Volatile anesthetics enhance flash-induced gamma oscillations in rat visual cortex. Anesthesiology. 2005; 102:937–947. [PubMed: 15851880]

Kenny JD, Westover MB, Ching S, Brown EN, Solt K. Propofol and sevoflurane induce distinct burst suppression patterns in rats. Front Syst Neurosci. 2014; 8:237. [PubMed: 25565990]

Koch C, Massimini M, Boly M, Tononi G. Neural correlates of consciousness: progress and problems. Nat Rev Neurosci. 2016; 17:307–321. [PubMed: 27094080]

Koenig T, Prichep L, Lehmann D, Sosa PV, Braeker E, Kleinlogel H, Isenhart R, John ER. Millisecond by millisecond, year by year: normative EEG microstates and developmental stages. NeuroImage. 2002; 16:41–48. [PubMed: 11969316]

Kroeger D, Amzica F. Hypersensitivity of the anesthesia-induced comatose brain. J Neurosci. 2007; 27:10597–10607. [PubMed: 17898231]

Lamme VA, Roelfsema PR. The distinct modes of vision offered by feedforward and recurrent processing. Trends Neurosci. 2000; 23:571–579. [PubMed: 11074267]

Lee U, Oh G, Kim S, Noh G, Choi B, Mashour GA. Brain networks maintain a scale-free organization across consciousness, anesthesia, and recovery: evidence for adaptive reconfiguration. Anesthesiology. 2010; 113:1081–1091. [PubMed: 20881595]

Lee U, Ku S, Noh G, Baek S, Choi B, Mashour GA. Disruption of frontal-parietal communication by ketamine, propofol, and sevoflurane. Anesthesiology. 2013; 118:1264–1275. [PubMed: 23695090]

Lehmann D, Strik WK, Henggeler B, Koenig T, Koukkou M. Brain electric microstates and momentary conscious mind states as building blocks of spontaneous thinking: I. Visual imagery and abstract thoughts. Int J Psychophysiol. 1998; 29:1–11. [PubMed: 9641243]

Lewis LD, Weiner VS, Mukamel EA, Donoghue JA, Eskandar EN, Madsen JR, Anderson WS, Hochberg LR, Cash SS, Brown EN, Purdon PL. Rapid fragmentation of neuronal networks at the onset of propofol-induced unconsciousness. Proc Natl Acad Sci U S A. 2012; 109:E3377–E3386. [PubMed: 23129622]

Liu X, Lauer KK, Ward BD, Rao SM, Li SJ, Hudetz AG. Propofol disrupts functional interactions between sensory and high-order processing of auditory verbal memory. Hum Brain Mapp. 2012; 33:2487–2498. [PubMed: 21932265]

Liu X, Ward BD, Binder JR, Li SJ, Hudetz AG. Scale-free functional connectivity of the brain is maintained in anesthetized healthy participants but not in patients with unresponsive wakefulness syndrome. PLoS One. 2014; 9:e92182. [PubMed: 24647227]

Luczak A, Bartho P, Harris KD. Spontaneous events outline the realm of possible sensory responses in neocortical populations. Neuron. 2009; 62:413–425. [PubMed: 19447096]

Luczak A, McNaughton BL, Harris KD. Packet-based communication in the cortex. Nat Rev Neurosci. 2015; 16:745–755. [PubMed: 26507295]

Lukatch HS, Kiddoo CE, Maciver MB. Anesthetic-induced burst suppression EEG activity requires glutamate-mediated excitatory synaptic transmission. Cereb Cortex. 2005; 15:1322–1331. [PubMed: 15647528]

Maksimow A, Silfverhuth M, Langsjo J, Kaskinoro K, Georgiadis S, Jaaskelainen S, Scheinin H. Directional connectivity between frontal and posterior brain regions is altered with increasing concentrations of propofol. PLoS One. 2014; 9:e113616. [PubMed: 25419791]

Martuzzi R, Ramani R, Qiu M, Rajeevan N, Constable RT. Functional connectivity and alterations in baseline brain state in humans. NeuroImage. 2010; 49:823–834. [PubMed: 19631277]

Mashour GA. Top-down mechanisms of anesthetic-induced unconsciousness. Front Syst Neurosci. 2014; 8:115. [PubMed: 25002838]

Massobrio P, de Arcangelis L, Pasquale V, Jensen HJ, Plenz D. Criticality as a signature of healthy neural systems. Front Syst Neurosci. 2015; 9:22. [PubMed: 25762904]

Meyer K. The role of dendritic signaling in the anesthetic suppression of consciousness. Anesthesiology. 2015; 122:1415–1431. [PubMed: 25901843]

Moddemeijer R. On estimation of entropy and mutual information of continuous distributions. Signal Process. 1989; 16:223–248.

Monti MM, Lutkenhoff ES, Rubinov M, Boveroux P, Vanhaudenhuyse A, Gosseries O, Bruno MA, Noirhomme Q, Boly M, Laureys S. Dynamic change of global and local information processing in propofol-induced loss and recovery of consciousness. PLoS Comput Biol. 2013; 9:e1003271. [PubMed: 24146606]

Muir T. Note on selected combinations. Proc R Soc Edinb. 1902; 24:102–104.

Murphy M, Bruno MA, Riedner BA, Boveroux P, Noirhomme Q, Landsness EC, Brichant JF, Phillips C, Massimini M, Laureys S, Tononi G, Boly M. Propofol anesthesia and sleep: a high-density EEG study. Sleep. 2011; 34:283A–291A. [PubMed: 21358845]

Nasrallah FA, Lew SK, Low AS, Chuang KH. Neural correlate of resting-state functional connectivity under alpha2 adrenergic receptor agonist, medetomidine. NeuroImage. 2014; 84:27–34. [PubMed: 23948809]

Ogawa T, Shingu K, Shibata M, Osawa M, Mori K. The divergent actions of volatile anaesthetics on background neuronal activity and reactive capability in the central nervous system in cats. Can J Anaesth. 1992; 39:862–872. [PubMed: 1288911]

Oizumi M, Albantakis L, Tononi G. From the phenomenology to the mechanisms of consciousness: Integrated Information Theory 3.0. PLoS Comput Biol. 2014; 10:e1003588. [PubMed: 24811198]

Oizumi M, Amari S, Yanagawa T, Fujii N, Tsuchiya N. Measuring Integrated Information from the Decoding Perspective. PLoS Comput Biol. 2016; 12:e1004654. [PubMed: 26796119]

Pal D, Hambrecht-Wiedbusch VS, Silverstein BH, Mashour GA. Electroencephalographic coherence and cortical acetylcholine during ketamine-induced unconsciousness. Br J Anaesth. 2015; 114:979–989. [PubMed: 25951831]

Palanca BJ, Mitra A, Larson-Prior L, Snyder AZ, Avidan MS, Raichle ME. Resting-state functional magnetic resonance imaging correlates of sevoflurane-induced unconsciousness. Anesthesiology. 2015; 123:346–356. [PubMed: 26057259]

Paxinos, G.; Watson, C. The rat brain in stereotaxic coordinates. San Diego: Academic Press; 1998.

Petermann T, Thiagarajan TC, Lebedev MA, Nicolelis MA, Chialvo DR, Plenz D. Spontaneous cortical activity in awake monkeys composed of neuronal avalanches. Proc Natl Acad Sci U S A. 2009; 106:15921–15926. [PubMed: 19717463]

Pillay S, Vizuete J, Liu X, Juhasz G, Hudetz AG. Brainstem stimulation augments information integration in the cerebral cortex of desflurane-anesthetized rats. Front Integr Neurosci. 2014; 8:8. [PubMed: 24605091]

Prichard D, Theiler J. Generating surrogate data for time series with several simultaneously measured variables. Phys Rev Lett. 1994; 73:951–954. [PubMed: 10057582]

Rampil IJ, Lockhart SH, Eger EI 2nd, Yasuda N, Weiskopf RB, Cahalan MK. The electroencephalographic effects of desflurane in humans. Anesthesiology. 1991; 74:434–439. [PubMed: 2001021]

Raz A, Grady SM, Krause BM, Uhlrich DJ, Manning KA, Banks MI. Preferential effect of isoflurane on top-down vs. bottom-up pathways in sensory cortex. Front Syst Neurosci. 2014; 8:191. [PubMed: 25339873]

Ribeiro TL, Copelli M, Caixeta F, Belchior H, Chialvo DR, Nicolelis MA, Ribeiro S. Spike avalanches exhibit universal dynamics across the sleep-wake cycle. PLoS One. 2010; 5:e14129. [PubMed: 21152422]

Robson JG. The effects of anesthetic drugs on cortical units. Anesthesiology. 1967; 28:144–154. [PubMed: 6017423]

Sarasso S, Boly M, Napolitani M, Gosseries O, Charland-Verville V, Casarotto S, Rosanova M, Casali AG, Brichant JF, Boveroux P, Rex S, Tononi G, Laureys S, Massimini M. Consciousness and complexity during unresponsiveness induced by propofol, xenon, and ketamine. Curr Biol. 2015; 25:3099–3105. [PubMed: 26752078]

Schrouff J, Perlbarg V, Boly M, Marrelec G, Boveroux P, Vanhaudenhuyse A, Bruno MA, Laureys S, Phillips C, Pelegrini-Issac M, Maquet P, Benali H. Brain functional integration decreases during propofol-induced loss of consciousness. NeuroImage. 2011; 57:198–205. [PubMed: 21524704]

Scott G, Fagerholm ED, Mutoh H, Leech R, Sharp DJ, Shew WL, Knopfel T. Voltage imaging of waking mouse cortex reveals emergence of critical neuronal dynamics. J Neurosci. 2014; 34:16611–16620. [PubMed: 25505314]

Sellers KK, Bennett DV, Hutt A, Frohlich F. Anesthesia differentially modulates spontaneous network dynamics by cortical area and layer. J Neurophysiol. 2013; 110:2739–2751. [PubMed: 24047911]

Sellers KK, Bennett DV, Hutt A, Williams JH, Frohlich F. Awake versus anesthetized: layer-specific sensory processing in visual cortex and functional connectivity between cortical areas. J Neurophysiol. 2015 00923:02014.

Shew WL, Yang H, Petermann T, Roy R, Plenz D. Neuronal avalanches imply maximum dynamic range in cortical networks at criticality. J Neurosci. 2009; 29:15595–15600. [PubMed: 20007483]

Sleigh JW, Vizuete JA, Voss L, Steyn-Ross A, Steyn-Ross M, Marcuccilli CJ, Hudetz AG. The electrocortical effects of enflurane: experiment and theory. Anesth Analg. 2009; 109:1253–1262. [PubMed: 19762755]

Solovey G, Alonso LM, Yanagawa T, Fujii N, Magnasco MO, Cecchi GA, Proekt A. Loss of consciousness is associated with stabilization of cortical activity. J Neurosci. 2015; 35:10866–10877. [PubMed: 26224868]

Steriade M, Amzica F, Contreras D. Cortical and thalamic cellular correlates of electroencephalographic burst-suppression. Electroencephalogr Clin Neurophysiol. 1994; 90:1–16. [PubMed: 7509269]

Tagliazucchi E, Chialvo DR, Siniatchkin M, Amico E, Brichant JF, Bonhomme V, Noirhomme Q, Laufs H, Laureys S. Large-scale signatures of unconsciousness are consistent with a departure from critical dynamics. J R Soc Interface. 2016:13.

Tononi G. Integrated information theory of consciousness: an updated account. Arch Ital Biol. 2012; 150:293–329. [PubMed: 23802335]

Tononi G, Boly M, Massimini M, Koch C. Integrated information theory: from consciousness to its physical substrate. Nat Rev Neurosci. 2016; 17:450–461. [PubMed: 27225071]

Touboul J, Destexhe A. Can power–law scaling and neuronal avalanches arise from stochastic dynamics? PLoS One. 2010; 5:e8982. [PubMed: 20161798]

Villeneuve MY, Casanova C. On the use of isoflurane versus halothane in the study of visual response properties of single cells in the primary visual cortex. J Neurosci Methods. 2003; 129:19–31. [PubMed: 12951229]

Vizuete JA, Pillay S, Diba K, Ropella KM, Hudetz AG. Monosynaptic functional connectivity in cerebral cortex during wakefulness and under graded levels of anesthesia. Frontiers in Integrative Neuroscience. 2012:6. [PubMed: 22375106]

Vizuete JA, Pillay S, Ropella KM, Hudetz AG. Graded defragmentation of cortical neuronal firing during recovery of consciousness in rats. Neuroscience. 2014; 275:340–351. [PubMed: 24952333]

Warnaby CE, Seretny M, Ni Mhuircheartaigh R, Rogers R, Jbabdi S, Sleigh J, Tracey I. Anesthesia-induced suppression of human dorsal anterior insula responsivity at loss of volitional behavioral response. Anesthesiology. 2016; 124:766–778. [PubMed: 26808631]

Werner G. Consciousness related neural events viewed as brain state space transitions. Cogn Neurodyn. 2009a; 3:83–95. [PubMed: 19003465]

Werner G. Viewing brain processes as critical state transitions across levels of organization: neural events in cognition and consciousness, and general principles. Biosystems. 2009b; 96:114–119. [PubMed: 19124060]

White EP, Enquist BJ, Green JL. On estimating the exponent of power–law frequency distributions. Ecology. 2008; 89:905–912. [PubMed: 18481513]

APPENDIX A. SUPPLEMENTARY DATA

Supplementary data associated with this article can be found, in the online version, at http://dx.doi.org/10.1016/j.neuroscience.2016.10.023.

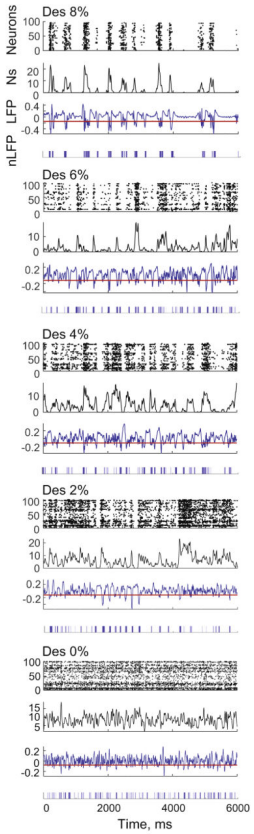

Fig. 1.

An example of unit and LFP activity in rat visual cortex at four states of anesthesia and wakefulness in one rat. Spiking activity of approximately 100 neurons was recorded with a 64-site microelectrode array. In raster plot (top), each dot represents an extracellular spike. The number of spikes (Ns, below) in 10-ms bins from all neurons are plotted after 5-point weighted linear polynomial smoothing. The LFP trace is from data sampled at 100 Hz to match 10-ms bin spike counts. Binary nLFP events (bottom trace) are obtained at mean minus 1 standard deviation, red line shows this threshold. Desflurane concentration (%) is shown on top of each panel. The close temporal correlation between population spiking and nLFP is evident at all levels of anesthesia in spite of difference in overall spike rate and temporal pattern. Strongly intermittent unit activity in deep anesthesia (8%) is gradually transformed to nearly continuous activity en route to wakefulness. (For interpretation of the references to color in this figure legend, the reader is referred to the web version of this article.)

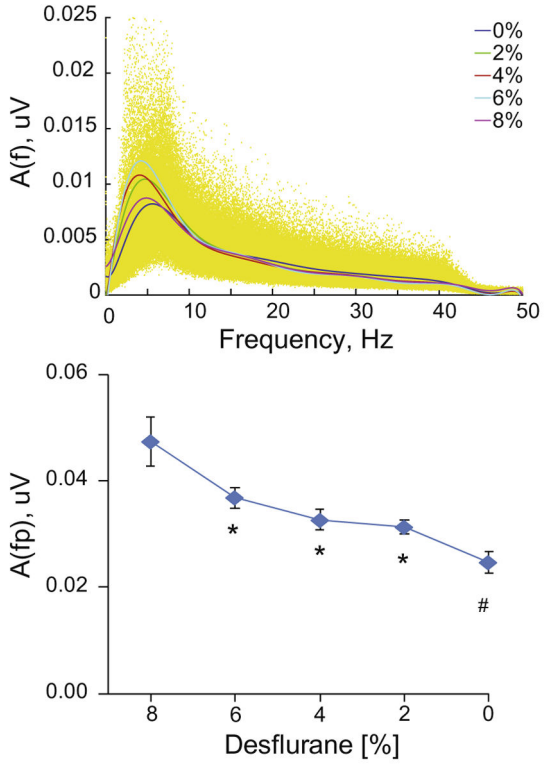

Fig. 2.

Amplitude spectra of LFP from all recording sites and animals at five desflurane concentrations indicated in%. Individual data are shown in yellow (top panel). Peak amplitude as a function of desflurane (bottom panel). $^{*}p<0.05$ vs. 8%, $^{\#}p<0.05$ vs. 8% and 6% (T-K).

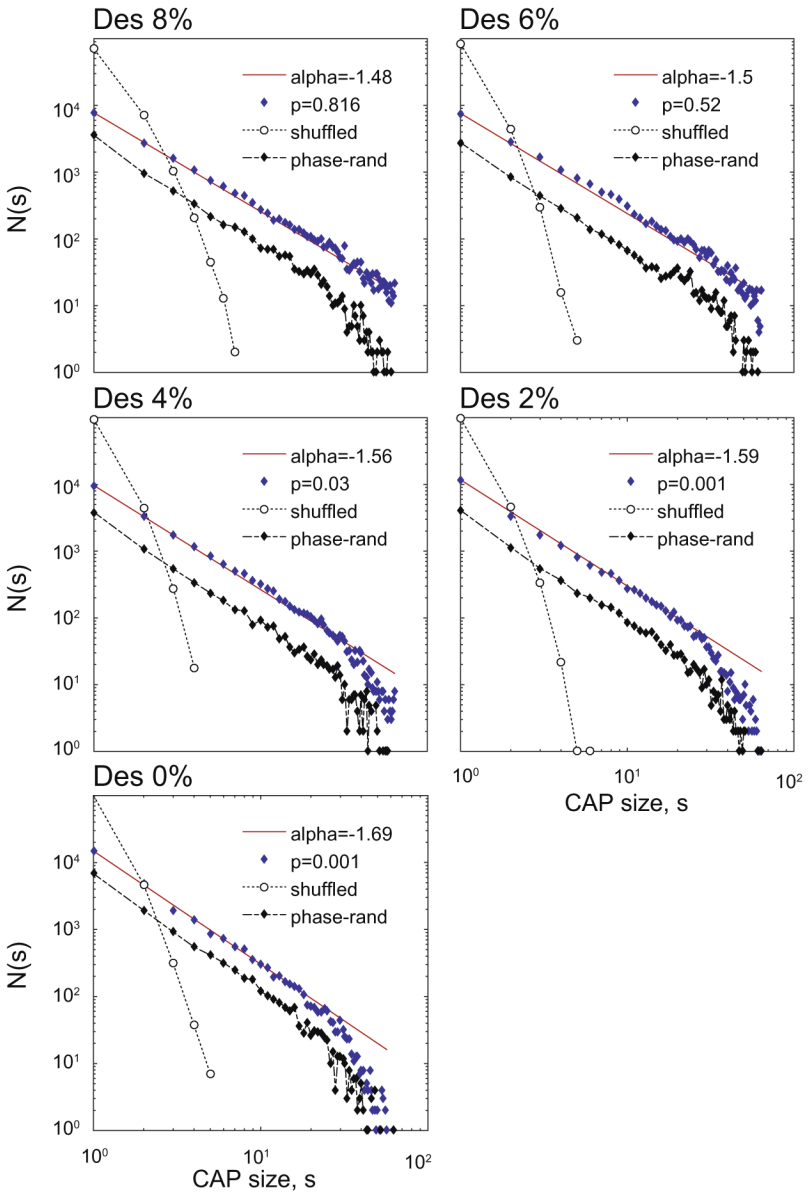

Fig. 3.

Distribution of CAP size in five states (anesthetic concentration indicated on top of each panel). CAP size s at each time point is included in the counts N(s). Data are pooled from twelve rats. Straight line (red) corresponds to power–law fit with slope alpha. The p value is from the K–S test. The number of large CAPs gradually drops below those predicted by power–law as the animals regain wakefulness. Shuffling the nLFP data diminishes CAPs larger than two and destroys the power–law (dotted line). Phase-randomization of LFP signal prior to thresholding does not change the power–law of CAP size distribution (dash-dotted line). (For interpretation of the references to color in this figure legend, the reader is referred to the web version of this article.)

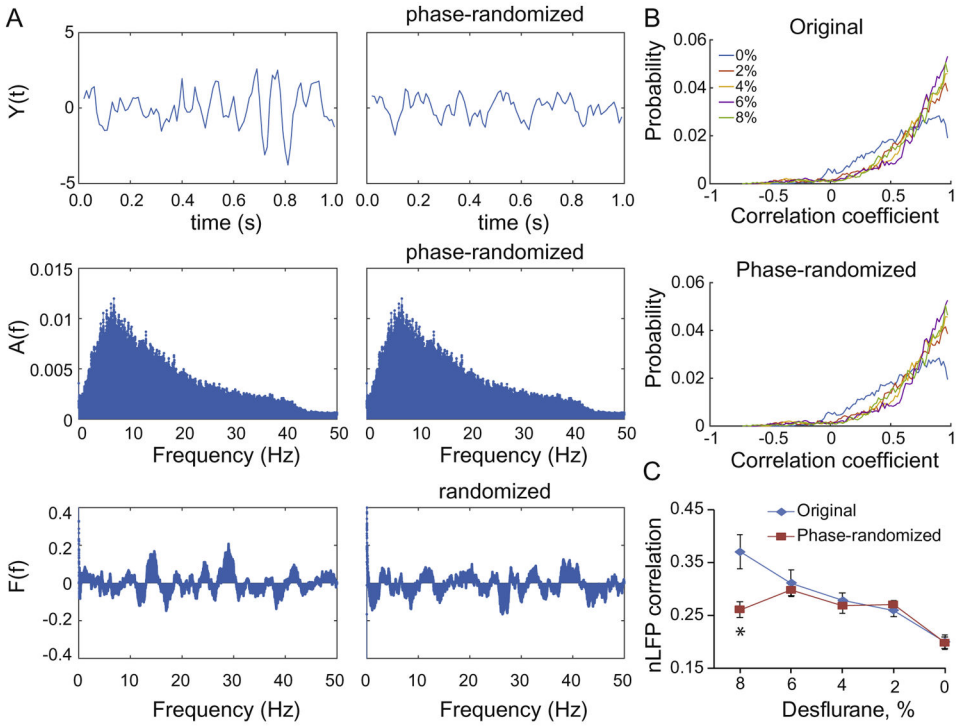

Fig. 4.

Effect of phase-randomization on nLFP correlations. (**A**) Steps of the analysis. The original signal (top left) is Fourier transformed to yield amplitude spectrum $A(f)$ and phase spectrum $F(t)$. Randomization of the phase at each frequency yields a new phase spectrum (bottom right) while the amplitude spectrum is conserved (middle right). The inverse Fourier transform yields a phase-randomized signal that looks different from the original (top right). The top panels show a short sample of the signal; spectra are from the entire 6-min segment. (B) Probability distribution of all pair-wise correlation coefficients of the LFP signals at five desflurane concentrations from the original and phase-randomized signals. (C) Average cross-correlation of nLFPs from all rats in each state. Original and phase-randomized data differ at 8% desflurane only. $^{*}p$=0.00066.

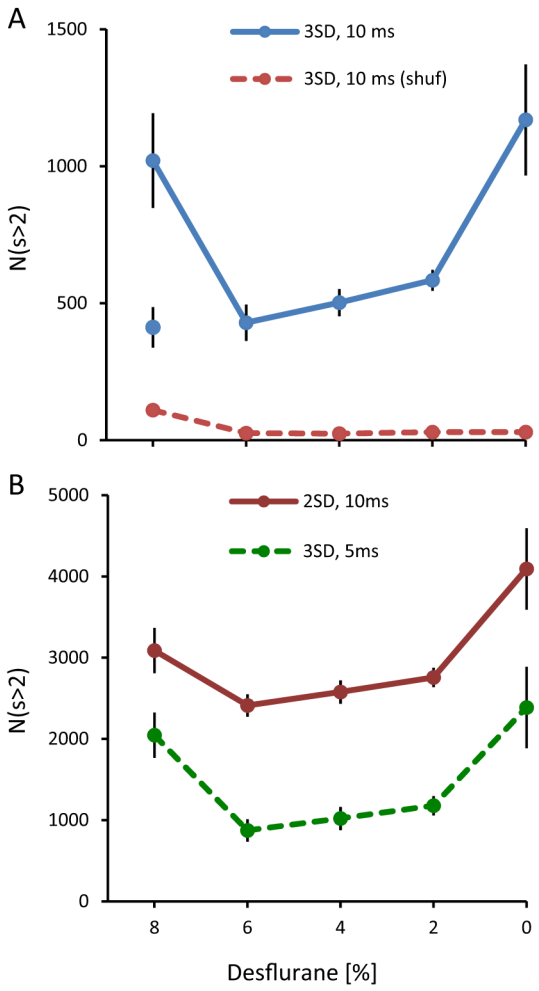

Fig. 5.

Summary statistics of CAPs (size >2) in rat visual cortex. (**A**) Total number of CAPs shows U-shape dependence on anesthetic depth. The number of CAPs is significantly elevated at 8% and 0% desflurane. $^{*}p < 0.05$ vs. 6%, 4% and 2% (T-K). Separate, unconnected symbol at 8% shows data from four animals that show no burst-suppression. There is no significant difference among the intermediate levels. (B) Number of CAPs calculated from nLFPs thresholded at different standard deviation (2SD, 3SD) or sampled at different time increments (5 ms, 10 ms). The results are similar to those in panel A.

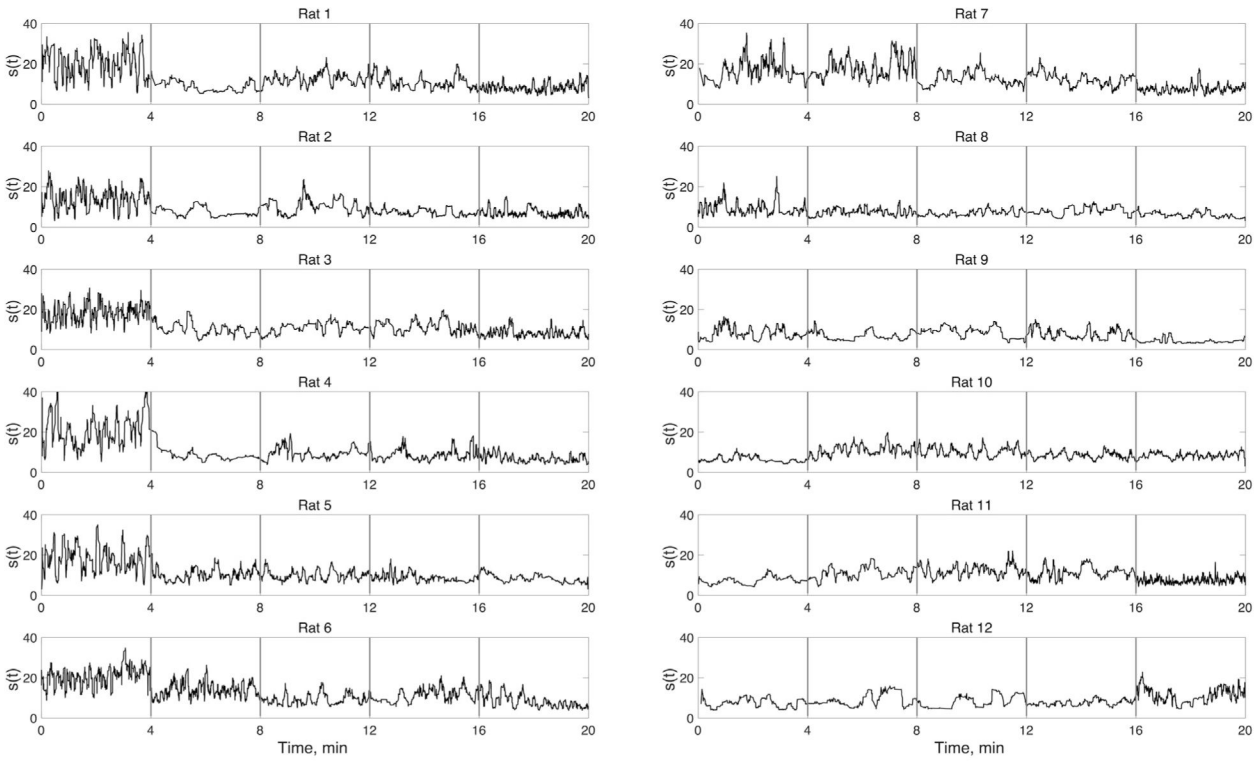

Fig. 6.

Variation in the size $s(t)$ of CAPs as a function of time across five conditions from 8% to 0% desflurane left to right (not indicated in figure). Vertical gray bars separate 4-min of data obtained in each condition. (The time scale is cumulative for the displayed data only; intervening periods are omitted.) Note the relatively large fluctuation of cluster size in rats that have burst-suppression at 8% desflurane (0–4 min, rats 1–8). The fluctuations are most suppressed during wakefulness (16–20 min).

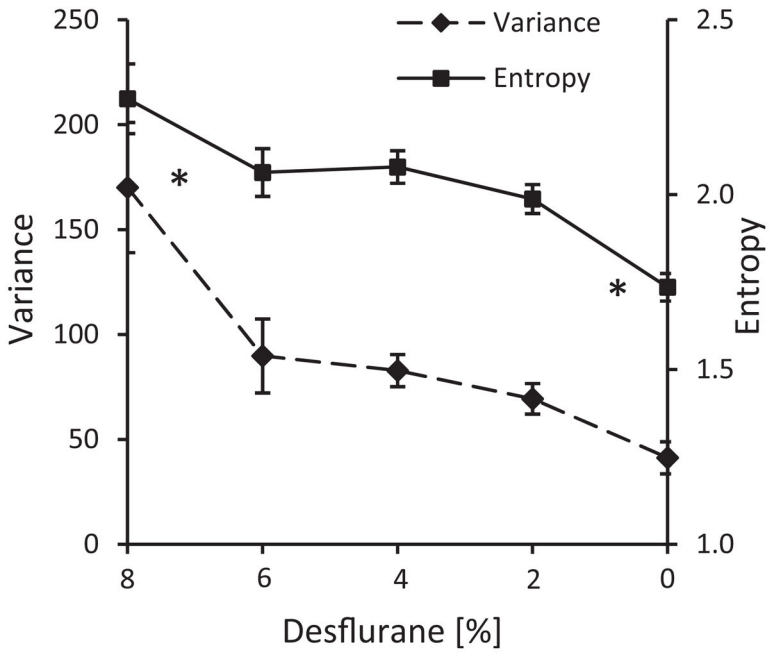

Fig. 7.

Dependence of CAP size variance (A) and entropy (B) on desflurane concentration. There is no difference near the recovery of consciousness, between 6% and 4% desflurane. $^{*}p<0.05$ vs. all other levels combined.

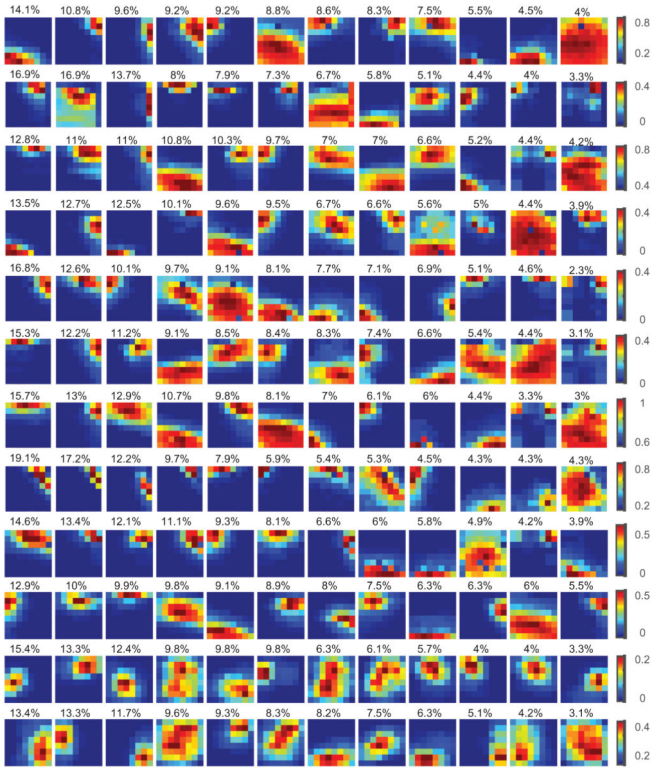

Fig. 8.

Typical landscapes of spatially correlated spontaneous population activity in rat visual cortex as indicated by local clusters (CAPs) of negative LFP deviations (nLFP). LFP data were recorded by a two-dimensional 8 − 8 multielectrode array. Data from five anesthetic conditions were concatenated and CAPs with size >2 at each time point were classified into 12 types by K-means clustering. Plots in each row show the average landscape of CAPs in 12 clusters arranged in descending order of the number of CAPs contained (percentage of CAPs shown on top of the panels). Pseudo-color corresponds to the probability of a site being a member of the corresponding CAP. The orientation of sites in each color plot is rostrocaudal (left–right) and dorsoventral (top-down). Each row is from a different rat.

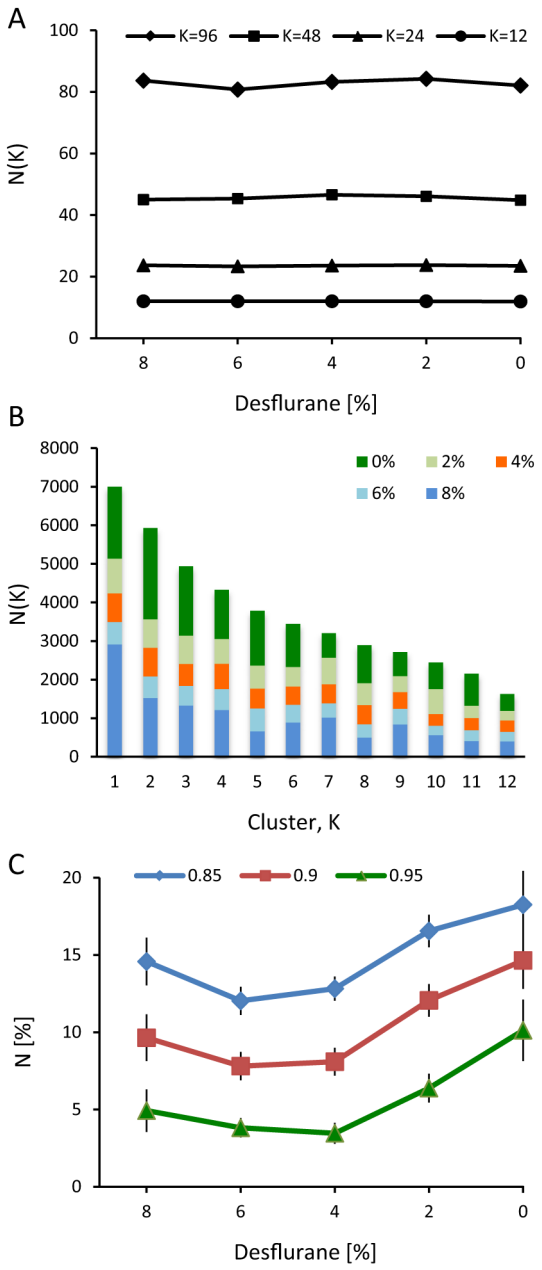

Fig. 9.

Results from CAP clustering as a function of state. (A) Number of CAP types (*N*(*K*)) present in each anesthetic condition at different cluster numbers *K*. *K*-means clustering was done on concatenated data and then the CAP types were counted in each condition. Virtually all cluster types occur in all states. (B) Number of CAPs *N*(*K*) in 12 clusters *K*. Anesthetic concentration is indicated in the legend. Data were combined from all animals, after ordering the 12 clusters according to the number of CAPs contained. Certain clusters contain disproportionally more CAPs at 8% and 0% desflurane than the rest. (C) Number of CAP centers that spatially cluster together at three smoothness thresholds. Clustering tendency is

the highest in wakefulness but not different among the other states, particularly near the transition between unconsciousness (6%) and consciousness (4%).

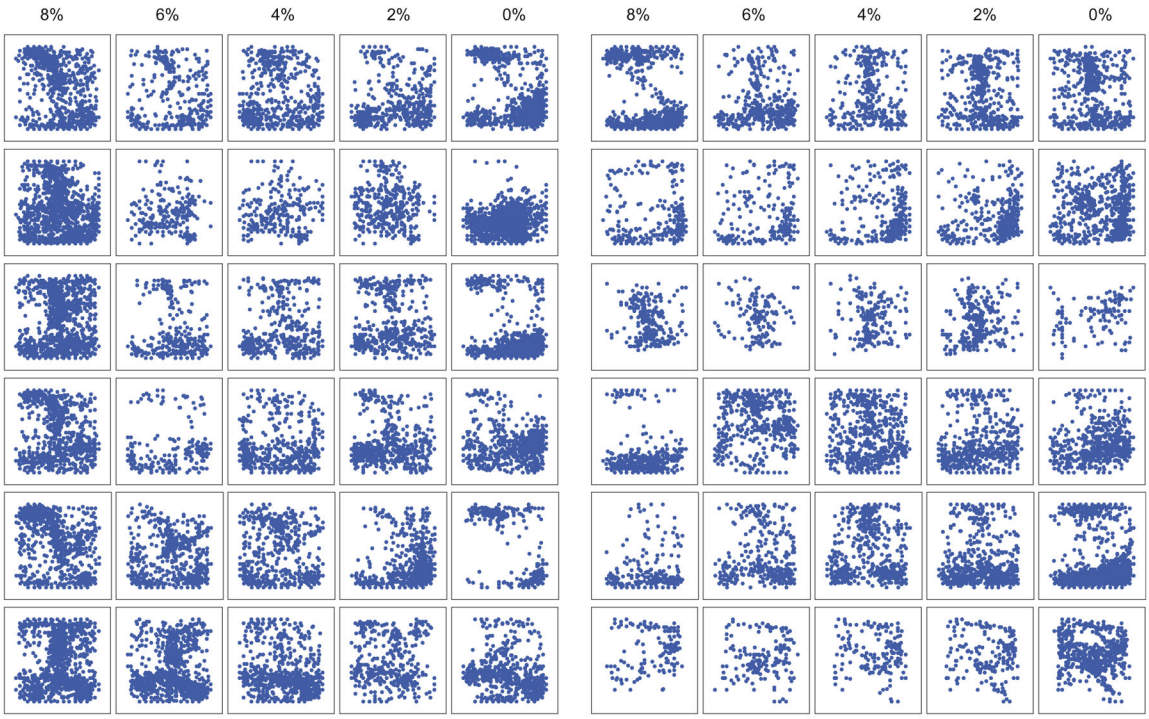

Fig. 10.

Center coordinates of CAPs in the visual cortex of twelve rats (arranged in the same order as in Fig. 4) in five states (anesthetic concentration indicated on top). Numbers by the axes indicate recording sites (*X* axis: rostrocaudal, *Y* axis: dorsoventral). CAP centers tend to segregate in different regions of the recording field that change with state in each animal.

Table 1

Burst-suppression ratio (BSR, %) in twelve rats

Desflurane (%)	Rat 1	Rat 2	Rat 3	Rat 4	Rat 5	Rat 6
8	69	59	56	75	74	73
6	0	0	0	0	4	13
	Rat 7	Rat 8	Rat 9	Rat 10	Rat 11	Rat 12
8	15	14	0	0	3	3
6	14	1	0	0	0	0